Oncology
and Radiotherapy©
18 (8) 2024: 001-007 • REVIEW ARTICLE

Efficient radio surgery segmentation of different brain tumors using deep learning

Vijay Upadhye[1], Tarang Bhatnagar[2], Avadhesh Kumar[3], Iype Cherian[4], Sandeep Kumar C[5], Shikhar Gupta[6]

[1] Department of Microbiology, Parul University, Vadodara, Gujarat, India
[2] Centre of Research Impact and Outcome, Chitkara University, Rajpura, Punjab, India
[3] Department of Computer Science and Engineering, Galgotias University, Greater Noida, Uttar Pradesh, India
[4] Institute of Neurosciences, Rajinder Nagar, New Delhi, India
[5] Department of Genetics, School of Sciences, JAIN (Deemed-to-be University), Karnataka, India
[6] Chitkara Centre for Research and Development, Chitkara University, Himachal Pradesh, India

ABSTRACT

Background: A feature of medical image processing poses a significant barrier in brain tumor segmentation. Patients' chances of receiving effective therapy and of surviving their brain tumors are greatly enhanced by early diagnosis. Separating brain tumors by hand from the enormous amount of MRI images produced in clinical practice to make a cancer diagnosis is a difficult and time-consuming task. Deep Learning (DL) models are being used to categorize medical pictures semantically at a quick pace.

Methods: In this work, used clinical stereotactic radio surgical dataset as a baseline to compare cutting-edge DL segmentation methods. Herein, proposed a novel DL based Hyper Automated Densely Fused Convolutional Neural Network (HADF-CNN) approach for brain tumor segmentation. To analyze the efficiency of the proposed method, initially, data were collected and preprocessed using Median Filter (MF) to remove unwanted noise. Next, the brain data is segmented using the suggested methodology. The categorization of brain tumors is done using the Deep Support Vector Machine (DSVM).

Results: To compared the proposed model performance with certain conventional segmentation methods. According to experimental data, the suggested approach performs better than traditional approaches.

Conclusion: Based on the data in this study, might draw the conclusion that DL has potential to help with brain lesion segmentation.

Keywords: deep learning, image segmentation, brain tumors, radio surgery, Hyper Automated Densely Fused Convolutional Neural Network (HADF-CNN), Deep Support Vector Machine (DSVM)

Address for correspondence:
Vijay Upadhye
Department of Microbiology, Parul University, Vadodara, Gujarat, India
E-mail: vijay.upadhye82074@paruluniversity.ac.in

Word count: 3898 **Tables:** 04 **Figures:** 04 **References:** 30

Received: 14 August, 2024, Manuscript No. OAR-24-145460
Editor assigned: 17 August, 2024, Pre-QC No. OAR-24-145460(PQ)
Reviewed: 01 September, 2024, QC No. OAR-24-145460(Q)
Revised: 08 September, 2024, Manuscript No. OAR-24-145460(R)
Published: 16 September, 2024, Invoice No. J-145460

INTRODUCTION

Stereotactic Radio Surgery (SRS) is a technique for treating tumors and other problems with the spine, lungs, liver, brain, neck, and other body parts by using a large number of perfectly focused radiation beams [1]. Instead, stereotactic radio surgery employs 3D imaging to precisely target high radiation doses to the afflicted region with little to no influence on the healthy tissue around it [2]. The brain and spine are routinely treated using stereotactic radio surgery in a single session. Lung, liver, adrenal, and other soft tissue malignancies are treated using body radio surgery, and therapy often entails many (3 to 5) sessions. Stereotactic Body Radiation (SBRT) or Stereotactic Ablative Radiotherapy (SABR) are alternate names for stereotactic radio surgery, which is a technique used to treat cancers beyond the brain. High-energy radiation is used in radiosurgery to eradicate cancers and other disorders [3]. Radiation beams are dismissed at your brain from equipment outside of your body. Beams with very high doses are used in radio surgery in order to destroy all the cells in the target region. To prevent harming healthy cells, the beams are precisely targeted and tightly focused. It is often administered as an isolated treatment on a single day, but it may also be divided into 2 to 5 sessions spread out over a week [4]. In place of open brain surgery, which needs an incision, radio surgery may be utilized. For treatment choices to be more successful and for patients to survive, brain tumors must be detected early. Brain tumors are difficult and time-consuming to physically identify from the many MRI image produced by standard clinical practice when diagnosing cancer [5]. Automatic brain tumor image segmentation is required. The article's goal is to provide an overview of techniques for brain tumor segmentation using MRI data. Due to their cutting-edge results and superior efficacy in resolving the problem compared to earlier strategies, DL algorithms have lately acquired appeal for automated segmentation [6]. DL techniques may be used to efficiently handle and objectively assess the massive amounts of MRI-based image data. Numerous review articles have previously been written about conventional techniques for segmenting MRI-based brain tumor images. Unlike other articles, this one focuses on the area's most recent advancements in DL approaches. This section 1st gives a general review of brain tumors and how they are segmented [7]. These days, identifying brain tumors is an essential part of modern medical diagnosis [8]. For patients with brain tumors, early identification and tumor detection are crucial in order to increase patient survival. Due to the volumetric

richness of the scan sample, MRI identification of brain tumors for cancer therapy requires extensive processing [9]. Clinical data processing is labor-intensive and time-consuming. Early identification and precise segmentation of the brain tumor region are thus crucial [10]. Study described a Deep Neural Networks (DNN)-based technique for totally autonomous brain tumor segmentation [11]. The proposed networks fit both low-grade and high-grade glioblastomas seen in MR imaging. Paper provided a unique Support Vector Machines (SVM)-based method for autonomously segmenting the optic nerves [12]. The presented approach outperformed state-of-the-art techniques in terms of resilience, accuracy, and processing time, demonstrating a suitable trade-off between these 3 factors. The neural network is trained and evaluated using the Multimodal Brain Tumor Image Segmentation Benchmark (BraTS) competition dataset from 2017. The technique outperforms earlier studies, according on tests on datasets from the BraTS 2017 challenge [13]. Study examined several methods for MRI of the brain picture segmenting and detecting brain tumors [14]. Pre-processing stages are included in the phases for identifying brain tumors that have been addressed overall. Pre-processing includes a variety of processes, such as non-local diagnostic correction techniques, Markov random field techniques, and wavelet-based techniques. Research mentions that technique that expertly combines hand-crafted features with CNN is recommended for completely automated brain tumor segmentation [15]. Paper highlights the presentation of a DL-based method for separating brain cancers from several MRI modalities [16]. When predicting the output label, the optional hybrid convolutional neural network architecture considers both contextual and local input using a patch-based method. The study uses a fuzzy K-means technique in conjunction with an artificial neural network to identify the tumor area. It comprises four stages: Attribute extraction and selection, noise evacuation, and Segmentation and classification [17]. To reduce the susceptibility of the approach to noise, non-brain tissue is removed using morphological processes after adaptive Wiener filtering has been applied for denoising. Second, the Gaussian kernel-based fuzzy C-means method combined with K-means++ clustering is utilized to segment images [18]. Research provided a fully independent brain tumor diagnostic model using morphological dilation, hole-filling, and a parameter-free clustering technique [19]. The technique is applied to an axial slice of the training dataset for BRATS 2015 using the T1c modality. Article offered a way to plan radiation therapy for glioblastomas by dividing brain tumors and several organs in peril simultaneously [20]. The technique combines the use of convolutional limited whole-brain segmentation using Boltzmann machines combined with a contrast-adaptive generative model for tumor shape regularization [21].

In the study, an automated computer-based method for segmenting brain tumors is proposed. The network suggested in the article successfully defined the limits of the brain tumor area [22]. Study offered an automated profoundly Deep Neural Network (DNN) method for brain tumor segmentation using Magnetic Resonance Imaging (MRI) [23]. Employing the VGG-16 system, robust tumor segmentation was expert through application of Fully Convolution Networks (FCN) with transfer learning. To investigate the advancement of automated methods for glioma brain tumor segmentation. It is also crucial to use the benchmark to accurately compare different models. As a result, the BraTS challenges from 2012 to 2019 evaluate the most modern methods [24]. Study created and test a two-stage DL method called MetNet for segmenting brain metastases in MRI images taken prior to therapy [25]. Article employed a novel asymmetric UNet (asym-UNet) architecture to increase the precision of automated techniques used to identify Brain Metastases (BM) [26]. Possessing one up-sampling arm and 2 down-sampling arms, the end-to-end asymmetric 3D-UNet architecture was used to collect the images features. Work proposed an effective method that uses the threshold segmentation approach and then performs a few morphological procedures [27]. First, the quality of the MRI image is enhanced. Next, the pixels are divided into groups using threshold segmentation. Finally, the region of the picture containing the tumor with the highest intensity is determined using morphological operators.

MATERIALS AND METHODS

In this paper, used a clinical dataset from stereotactic radiosurgery to assess cutting-edge DL segmentation methods. Here, suggested a unique HADF-CNN strategy for dividing up brain tumors using DL segmentation. Figure 1 depicts the HADF-CNN process.

Dataset

The clinical stereotactic radio surgery, collected dataset were 2411 patients who underwent 2578 therapy courses. 2036 of these treatment regimens, involving 1921 individuals, were intracranial.

The patients included had access to contrast-enhanced T1-weighted (T1+C) MRI imaging and were receiving their first Software Requirements Specification (SRS). In the end, dataset had 1688 patients. Their data was arbitrarily divided into training and test sets (Table 1). However, because neither a tumor nor a vascular abnormality is appropriate therapeutic options for trigeminal neuralgia patients, all of their data were included in the training set.

The target and axial T1+C MRI were both taken out of the treatment planning system for each patient. The majority of the time, a radiation oncologist assessed the targets after a neurosurgeon contoured them. On occasion, the targets were contoured by a single radiation oncologist without a second doctor's evaluation. More than one target may be present in an imaging volume, especially in patients with brain metastases. Tumor contours were kept in CT coordinates after Prior to contouring, data volumes had been assigned to CT volumes. To convert the tumor labels into MRI coordinates, an inverse transformation was required. Alternatively put, volumes were resampled rather than immediately cropped on grids with various voxel counts. Names, birthdates, and location information were stripped from the images before they were recorded in Clinical diagnoses data format.

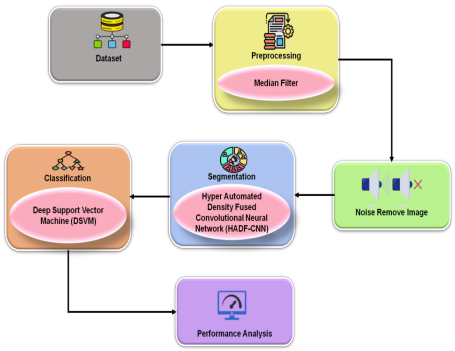

Fig. 1. Flow of the proposed methodology

Tab. 1. Clinical diagnosis in the final dataset for 1688 patients

Varieties of Brain Lesions	Train	Test
Metastases	504	55
Schwannoma	309	20
Meningioma	317	29
Arteriovenous malformation	83	6
Pituitary tumor	147	8
Other tumors	172	15
Trigeminal neuralgia	41	0
Total	1669	132

These image/label pairings used for instruction and assessing Deep Neural Networks (DNN) after registration and de-identification. With slice thicknesses of 1 mm-2 mm, the pictures were shown as native axial slices. Since the slices might occasionally only partially cover the region of interest, the number of slices ranged from 30 to 233. The lowest in-plane resolution was 197 × 197, while the average was 512 × 512. Typically, 300 mm in the x-y plane, however it might be as large as 350 mm. The majority of the pixels were 0.5859 mm^2 × 0.5859 mm^2, however some photos with lesser quality had pixels that were 1.1719 mm^2 × 1.1719 mm^2. These 1688 picture sets had a totally of 2568 different targets. The intended volumes ranged from 20,646,646 mm^3, with 3696 mm^3 for the mean and 6637 mm^3 for the median. There was a single target present throughout 1013 image sets. In a single image collection, there may be up to 34 targets.

Preprocessing median filter

The MF is a nonlinear signal processing technique with a statistical foundation. Since the median filter applies to images with random noise, it is a nonlinear filter that is challenging to analytically evaluate. A normal distribution image with zero mean noise has a very little noise variance in the MF.

$$\sigma_{med}^2 = \frac{1}{4me^2(\overline{m})} \approx \frac{\sigma_j^2}{m+\frac{\pi}{2}-1}\frac{\pi}{2} \quad (1)$$

Where σ_0^2 how big the MF mask is, σ_0^2 is input power of noise (the variance), and (me is function about noise density).

$$\sigma_0^2 = \frac{1}{m}\sigma_j^2 \quad (2)$$

By comparing (1) and (2), it is evident that the effect of median filtering is dependent on both the mask's size and the noise distribution. The median filter reduces random noise far better than average filtering, even if impulsive noise, particularly slender pulses, are spaced longer separately and have a reduced pulse width in comparison to 2/n. Given the capabilities of the average and median filtering algorithms of adjusting the mask size in response to the noise density, the performance of the median filtering should be enhanced.

Hyper Automated Densely Fused Convolutional Neural Network (HADF-CNN)

The issue of vanishing/exploding gradients is one that deep architectures have; this problem prevents convergence during training. The research in examined densely linked networks to address these issues in incredibly deep structures. Dense Nets work on the fundamental tenet that training is made easier and more effective when direct connections are established in a feed-forward manner from all layers to each subsequent layer. This is founded on three observations. Initially, given that every feature map in the design has a short path, a thorough supervision is implied. Second, the network's overall information flow and gradients are improved through direct connections between all levels. Third, the regularizing impact of dense connections is to lessen the probability of excessive fitting on issues with fewer training sets. Let v_{k-1}represent the 1[th] layer's output. This vector is often acquired from the preceding layer's output in CNNs.

$v_{k-1}$by a mapping v_k consisting of a non-linear activation function after a convolution:

$$v_k = G_k(v_{k-1}) \quad (3)$$

All feature outputs in a highly linked network are feed-forward concatenated.

$$v_k = G_k([v_{k-1}, v_{k-2,\ldots}v_{k-0}]), \quad (4)$$

Hyperdense Net extends this idea by adding a more comprehensive concept of connectedness, as join layer outputs from many streams, each of which is associated with a distinct type of visual procedure. Within the framework of several modes, the hyper automated densely fused CNN offers a feature representation that is far more powerful than early/late fusion because the network comprehends the intricate connections that exist within and among each level of encapsulation. While development to N modes is straightforward, let's concentrate on the situation of two picture modalities for simplicity's sake. Where, $v_{k-1}^1$and $vv_{k-2,}^2$stand for the 1th layer outputs in streams 3 and 4, respectively. Following is a general definition of the result of layer L in a stream:

$$v_k^t = G_k^t([v_{k-1}^1, v_{k-2,}^2 v_{k-2}^1, v_{k-2}^2, \ldots, v_0^1, v_0^2]) \quad (5)$$

Recent research has shown that reordering and interlacing the CNN's feature map components is a potent regularize that improves effectiveness and performance. In the process of deterministic adjustments to increase efficiency, intermediary CNN layers may, regrettably, lose some crucial information. To address this problem, intermediary layers should provide many channels of information exchange while maintaining the deterministic functions that were previously mentioned. This idea prompts us to join feature maps in a different order for every branch and layer.

$$v_k^t = G_k^t(\pi_k^t([v_{k-1}^1, v_{k-1}^2, v_{k-2}^2, \ldots, v_0^1, v_0^2])) \quad (6)$$

For instance, it may have two picture modalities and

$$v_k^1 = G_k^1([v_{k-1}^1, v_{k-1}^2, v_{k-1}^1, v_{k-2}^2, \ldots, v_0^1, v_0^2]) \quad (7)$$

The strong arrows depict the corresponding correlations among feature maps with various layers, inside and across the different streams, noting that only convolution operations are indicated by the red arrows. The outputs of all the prior layers from the G_k^1 route is concatenated to form each convolutional block's input. Next, a total about pseudo-randomly initialized SVM are present, each of which learns to extract one feature,v_{k-1}^2, from an input pattern, v_{k-1}^1. The primary support vector machine, or SVM, uses the extracted feature vector as input and tries to estimate the target function. To use the following methods to determine the input vector v_{k-1}^1 feature-layer representation:

$$v_k^1 = G_k^2([v_{k-1}^2, v_{k-1}^1, v_{k-1}^2, v_{k-2}^1, \ldots, v_0^2, v_0^1]) \quad (8)$$

The feature maps from different levels, both inside and outside of the numerous streams, are directly connected the red arrows only depict convolution processes, as opposed to the black arrows' representation.

Classification using Deep Support Vector Machine (DSVM)

The DSVM is a prominent type of machine learning algorithm for categorization issues. It's a variant of the conventional SVM technique, the input and output layers are combined with many non-linear transformation layers. A deep DSVM, every input data is first transformed through a series of non-linear transformations, which are typically implemented using neural network layers. A typical DSVM classifier receives the output from these layers, which makes the final prediction. The learning algorithm uses a min-max method to modify the DSVM co offends of all DSVMs.

Creating the dual objective W for the primary DSVM

$$\min_{g(v)}\max_{\alpha,\alpha*} U(g(v), \alpha^{(*)}) = -\varepsilon \sum_{j=1}^{k}(\alpha_j^* + \alpha_j) + \sum_{j=1}^{k}(\alpha_j^* + \alpha_j)z_j (9)$$

$$\frac{1}{2}\sum_{j,i=1}^{k}(\alpha_j^* + \alpha_j)(\alpha_i^* + \alpha_i)L\left(g(v_j), g(v_i)\right) \quad (10)$$

$\alpha^{(*)}$(Standing for all $\alpha_j^*$and α_j)toward a

(Local) maximum of U, where $\prec$ is the learning rate:

$$\alpha_j^{(*)} \leftarrow \alpha_j^{(*)} + \prec . \partial U / \partial \alpha_j^{(*)} \quad (11)$$

The resulting gradient ascent learning rule for α_j is:

$$\alpha_j = \alpha_j + \prec \left(-\epsilon - z_j + \sum_i \left(\alpha_j^{(*)} - \alpha_i\right) L\left(g(v_j), g(v_i)\right)\right. \quad (12)$$

$$L\left(g(v_j), g(v_i)\right) = \exp\left(-\sum_\alpha \frac{\left(g(v_j)_b, g(v_i)_b\right)^2}{\sigma_n}\right) \quad (13)$$

Utilizing a method analogous to back propagation, the system creates a fresh dataset for each feature layer DSVM

$$\left(v_j, g(v_j)_b - \mu . \frac{\delta U}{\delta e(v_j)_a}\right)$$

where denotes a learning rate,

$$\delta U / \delta e(v_j)_a \quad (14)$$

Is given by:

$$\frac{\delta U}{\delta e(v_j)_b} = \left(\alpha_i^* - \alpha_j\right)\left(g(v_j)_b, g(v_i)_b\right) \quad (15)$$

$$L\left(g(v_j)_b, g(v_i)_b\right) \quad (16)$$

The main DSVM and feature layer SVMs are trained alternately over several epochs after the feature extraction SVMs are pseudo-randomly started. The average mistakes are used to calculate the bias values.

RESULTS

Radio surgery is a treatment option for both small malignant and benign (noncancerous) brain tumors. Here, to contrast the suggested approach with a few of the current approaches, including Deeper ResU-net, RGB-D, and U-Net.

Dice coefficient

One mathematical measure that is frequently utilized in medical imaging is the dice coefficient, including the analysis of brain lesions. Specifically, the similarity between two sets of data is gauged using the Dice coefficient. The results of the suggested procedure are contrasted with those of the conventional techniques in figure 2 and table 2. Figure 2 shows that the dice of the recommended methodology are higher than those of the traditional ways.

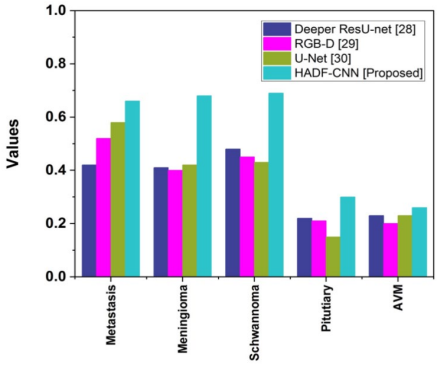

Fig. 2. Computation analysis of dice coefficient

Tab. 2. Computation analysis of dice coefficient

	Deeper ResU-net [28]	RGB-D [29]	U-Net [30]	HADF-CNN [Proposed]
Metastasis	0.42	0.52	0.58	0.66
Meningioma	0.41	0.4	0.42	0.68
Schwannoma	0.48	0.45	0.43	0.69
Pituitary	0.22	0.21	0.15	0.3
AVM	0.23	0.2	0.23	0.26

Sensitivity

The sensitivity is the proportion of actual positive results (for example, a sensitivity of 90% means that 90% of those who have brain tumor illness will test positive). The proportion of actual negative results is known as specificity (for example, ninety percent of individuals who do not possess the target ailment will test negative, according to the 90% specificity). The accuracy of the suggested strategy is contrasted with the conventional methods in figure 3 and table 3. In comparison to traditional approaches, figure 3 demonstrates that the suggested method has a higher sensitivity.

Precision

Precision in the context of brain tumors refers to the accuracy of a diagnostic or treatment method in identifying or targeting cancerous tissue while minimizing damage to healthy brain tissue. Table 4 presents a comparison between the precision of the suggested method and the conventional approaches. Figure 4 illustrates how the precision of the suggested technique is higher than that of traditional methods.

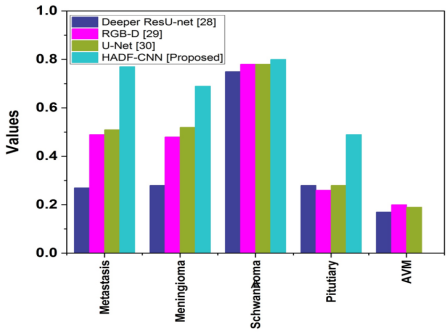

Fig. 3. Computation analysis of sensitivity

Tab. 3. Computation analysis of sensitivity

	Deeper ResU-net [28]	RGB-D [29]	U-NET [30]	HADF-CNN [Proposed]
Metastasis	0.27	0.49	0.51	0.77
Meningioma	0.28	0.48	0.52	0.69
Schwannoma	0.75	0.78	0.78	0.8
Pituitary	0.28	0.26	0.28	0.49
AVM	0.17	0.2	0.19	0.28

Tab. 4. Computation analysis of precision

	Deeper ResU-net [28]	RGB-D [29]	U-NET [30]	HADF-CNN [Proposed]
Metastasis	0.6	0.62	0.61	0.77
Meningioma	0.47	0.49	0.43	0.65
Schwannoma	0.46	0.43	0.59	0.6
Pituitary	0.2	0.24	0.41	0.45
AVM	0.23	0.25	0.43	0.58

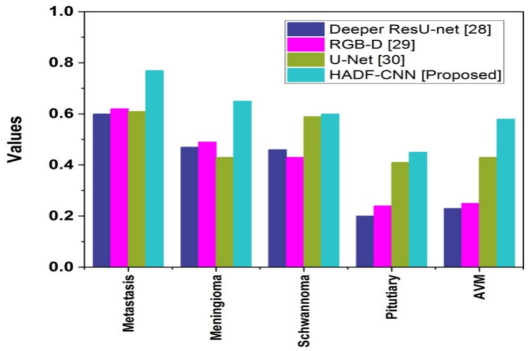

Fig. 4. Computation analysis of precision

CONCLUSIONS

In this study, suggested a hyper automated densely fused convolutional neural network to categorize brain tumors. To analyze the efficiency of the proposed method, data were gathered and preprocessed using median filter. Next, the brain data is segmented using the proposed method. The brain tumor categorization process makes use of the DSVM. The design of the proposed technique is comparable to CNN, but it uses less power and processes huge images in a reasonable amount of time. Additionally, compared to conventional classifiers, the proposed classifier demonstrates greater accuracy.

REFERENCES

1. Graber JJ, Cobbs CS, Olson JJ. Congress of neurological surgeons systematic review and evidence-based guidelines on the use of stereotactic radiosurgery in the treatment of adults with metastatic brain tumors. Neurosurgery. 2019;84;168-170.
2. Noori M, Bahri A, Mohammadi K. Attention-guided version of 2D UNet for automatic brain tumor segmentation. IEEE. 2019;269-275.
3. Voglhuber T, Kessel KA, Oechsner M, Vogel MM, Gschwend JE, et al. Single-institutional outcome-analysis of low-dose stereotactic body radiation therapy (SBRT) of adrenal gland metastases. BMC Cancer. 2020;20:1-9.
4. Ekhator C, Nwankwo I, Rak E, Homayoonfar A, Fonkem E, et al. GammaTile: Comprehensive review of a novel radioactive intraoperative seed-loading device for the treatment of brain tumors. Cureus. 2022;14;29970.
5. Chukwueke UN, Wen PY. Use of the Response Assessment in Neuro-Oncology (RANO) criteria in clinical trials and clinical practice. CNS Oncol. 2019;8.
6. Bhandari A, Koppen J, Agzarian M. Convolutional neural networks for brain tumour segmentation. Insights Imaging. 2020;11:1-9.
7. Chattopadhyay A, Maitra M. MRI-based brain tumor image detection using CNN based deep learning method. Neurosci Inform. 2022:100060.
8. D'hooghe MB, Gielen J, Van Remoortel A, D'haeseleer M, Peeters E. Single MRI□based volumetric assessment in clinical practice is associated with MS□related disability. J Magn Reson Imaging. 2019;49:1312-1321.
9. Rieke J, Eitel F, Weygandt M, Haynes JD, Ritter K. Visualizing convolutional networks for MRI-based diagnosis of Alzheimer's disease. Springer Int Publ. 2018; 24-31.
10. Bangalore Yogananda CG, Shah BR, Vejdani-Jahromi M, Nalawade SS, Murugesan GK. et al. A novel fully automated MRI-based deep-learning method for classification of IDH mutation status in brain gliomas. Neuro Oncol. 2020;22:402-411.
11. Havaei M, Davy A, Warde-Farley D, Biard A, Courville A. et al. Brain tumor segmentation with deep neural networks. Med Image Anal. 2017;35:18-31.
12. Dolz J, Leroy HA, Reyns N, Massoptier L, Vermandel M. A fast and fully automated approach to segment optic nerves on MRI and its application to radiosurgery. IEEE; 2015;1102-1105.
13. Pourreza R, Zhuge Y, Ning H, Miller R. Brain tumor segmentation in MRI scans using deeply-supervised neural networks. Springer Int. Publ. 2018;320-331.
14. Rani E, Grace Priya A, Indiranatchiyar A. Brain tumor detection using ANN classifier. Brain Tumor Detect Using ANN Classif. 2019;5.
15. Khan H, Shah PM, Shah MA, ul Islam S, Rodrigues JJ. Cascading handcrafted features and Convolutional Neural Network for IoT-enabled brain tumor segmentation. Comput Commun. 2020;153:196-207.
16. Sajid S, Hussain S, Sarwar A. Brain tumor detection and segmentation in MR images using deep learning. Arab J Sci Eng. 2019;44:9249-9261.
17. Rundo L, Militello C, Tangherloni A, Russo G, Vitabile S, et al. Next for neuro□radiosurgery: a fully automatic approach for necrosis extraction in brain tumor MRI using an unsupervised machine learning technique. Int J Imaging Syst Technol. 2018;28:21-37.
18. Zhang C, Shen X, Cheng H, Qian Q. Brain tumor segmentation based on hybrid clustering and morphological operations. Int J Biomed Imaging. 2019;2019:7305832.
19. Shivhare SN, Sharma S, Singh N. An efficient brain tumor detection and segmentation in MRI using parameter-free clustering. Springer Singapore. 2019;485-495.
20. Agn M, af Rosenschöld PM, Puonti O, Lundemann MJ, Mancini L. et al. A modality-adaptive method for segmenting brain tumors and organs-at-risk in radiation therapy planning. Med Image Anal. 2019;54:220-237.
21. Tripathi S, Sharan TS, Sharma S, Sharma N. Segmentation of brain tumour in MR images using modified deep learning network. IEEE;2021;1-5.
22. Agravat RR, Raval MS. A survey and analysis on automated glioma brain tumor segmentation and overall patient survival prediction. Arch Comput Method Eng. 2021;28:4117-4152.
23. Zhou Z, Sanders JW, Johnson JM, Gule-Monroe M, Chen M. et al. MetNet: Computer-aided segmentation of brain metastases in post-contrast T1-weighted magnetic resonance imaging. Radiother Oncol. 2020;153:189-196.
24. Cao Y, Vassantachart A, Jason CY, Yu C, Ruan D. et al. Automatic detection and segmentation of multiple brain metastases on magnetic resonance image using asymmetric UNet architecture. Phys Med Biol. 2021;66:015003.
25. Tarhini GM, Shbib R. Detection of brain tumor in MRI images using watershed and threshold-based segmentation. Int J Signal Process Syst. 2020;8:19-25.
26. Ivashchenko OV, Zhai Z, Stoel BC, Ruers TJ. Optimization of hepatic vasculature segmentation from contrast-enhanced MRI, exploring two 3D Unet modifications and various loss functions. SPIE; 2021;125-134.
27. Sahaai MB. Brain tumor detection using DNN algorithm. Turk J Comput Math Educ. 2021;12:3338-3345.
28. Yang T, Song J, Li L, Tang Q. Improving brain tumor segmentation on MRI based on the deep U-net and residual units. J Xray Sci Technol. 2020;28:95-110.
29. Deng W, Huang K, Chen X, Zhou Z, Shi C. et al. RGB-D based semantic SLAM framework for rescue robot. IEEE. 2020;6023-6028.
30. Ghosh S, Chaki A, Santosh KC. Improved U-Net architecture with VGG-16 for brain tumor segmentation. Phys Eng Sci Med. 2021;44:703-712.